THE JOURNAL OF BIOLOGICAL CHEMISTRY
Vol. 279, No. 6, Issue of February 6, pp. 4394–4403, 2004
Printed in U.S.A.

Nucleoside and RNA Triphosphatase Activities of Orthoreovirus Transcriptase Cofactor μ2*

Received for publication, August 5, 2003, and in revised form, October 21, 2003
Published, JBC Papers in Press, November 12, 2003, DOI 10.1074/jbc.M308637200

Jonghwa Kim‡§, John S. L. Parker‡¶, Kenneth E. Murray‡, and Max L. Nibert‡‖

From the ‡Department of Microbiology and Molecular Genetics, Harvard Medical School, Boston, Massachusetts 02115 and the §Department of Biochemistry, University of Wisconsin, Madison, Wisconsin 53706

The mammalian *Orthoreovirus* (mORV) core particle is an icosahedral multienzyme complex for viral mRNA synthesis and provides a delimited system for mechanistic studies of that process. Previous genetic results have identified the mORV μ2 protein as a determinant of viral strain differences in the transcriptase and nucleoside triphosphatase activities of cores. New results in this report provided biochemical and genetic evidence that purified μ2 is itself a divalent cation-dependent nucleoside triphosphatase that can remove the 5′ γ-phosphate from RNA as well. Alanine substitutions in a putative nucleotide binding region of μ2 abrogated both functions but did not affect the purification profile of the protein or its known associations with microtubules and mORV μNS protein *in vivo*. *In vitro* microtubule binding by purified μ2 was also demonstrated and not affected by the mutations. Purified μ2 was further demonstrated to interact *in vitro* with the mORV RNA-dependent RNA polymerase, λ3, and the presence of λ3 mildly stimulated the triphosphatase activities of μ2. These findings confirm that μ2 is an enzymatic component of the mORV core and may contribute several possible functions to viral mRNA synthesis.

The mammalian *Orthoreovirus* (mORV)[1] core particle is an icosahedral multienzyme complex for viral mRNA synthesis (for review, see Ref. 1–3). The core is released from the infectious virion during cell entry and is also formed from newly synthesized gene products as an assembly intermediate within infected cells. In addition to the 10 centrally condensed viral double-stranded RNA genome segments cores contain five different viral proteins in defined copy numbers (Table I). Virions contain three additional viral proteins that play key roles in particle stability and cell entry. The viral mRNAs are full-length plus-strand copies of the genome segments 1200–3900 nucleotides in length, modified by a dimethylated cap 1 structure at their 5′ ends and not polyadenylated. The manner in which the double-stranded RNA genome segments and mRNA products interact with the transcription and capping machinery in mORV cores is a topic of interest for understanding structural and mechanistic aspects of these processes in this and other viral and cellular systems.

X-ray crystallography has recently advanced our understanding of the core. A 3.6-Å crystal structure of the 52-MDa core particle has provided an atomic model for most residues of the three major core proteins: λ1 in the T = 1 shell, λ2 in the pentameric surface turrets, and σ2 in the monomeric surface nodules (4). Not visualized in that structure are the two stoichiometrically minor proteins, λ3 and μ2, which are located beneath the λ1 shell near the icosahedral 5-fold axes (5). To obtain an atomic model for λ3, which is the viral RNA-dependent RNA polymerase (6–8) and, thus, a functionally key element, a 2.5-Å crystal structure of recombinant λ3 has been determined (9). In addition, the λ3 structure has recently been fit into a 7.6-Å electron cryomicroscopy reconstruction of the mORV virion, revealing how λ3 associates with the λ1 shell (10). These studies leave μ2 as the only core protein for which no crystal structure is yet available (Table I). The roles of μ2 in core functions are also poorly defined.

Cores catalyze at least five different enzymatic reactions (Table I). In addition to the polymerase activity attributable to λ3, there are the four reactions in RNA 5′ capping: RNA 5′-triphosphatase (RTPase), guanylyltransferase, ^{7}N-methyltransferase, and $^{2'}O$-methyltransferase (3, 11). The RTPase activity has been assigned to the shell protein λ1 (12). The RNA guanylyl- and methyltransferases are contained in the turret protein λ2 (4, 13–18), through which the nascent transcripts are cotranscriptionally exported (19, 20). Cores also catalyze removal of the γ-phosphate group from NTPs (21–24). This activity might represent the RTPase, as observed with some other such enzymes (25–29), but might alternatively reflect a distinct activity not encompassed by the five reactions above. In fact, published findings suggest there may be two different types of nonspecific nucleoside triphosphatases (NTPases) in cores (23, 24). One of these NTPases might represent a core-associated RNA helicase that is involved in melting the double-stranded RNA genome segments during transcription (23, 24, 30), and indeed evidence for NTP-dependent RNA/DNA helicase activity by shell protein λ1 has been reported (30).

Two previous genetic studies have implicated μ2 in the enzymatic activities of cores. Yin *et al.* (31) show that the M1 genome segment, which encodes μ2, determines *in vitro* differences between cores of mORV strains type 1 Lang (T1L) and type 3 Dearing (T3D) in both the temperature optimum of transcription and the amounts of transcripts produced. Because λ3 is the viral polymerase (6–9), these genetic findings suggest an auxiliary role for μ2 in λ3 function. Noble and Nibert (24) show that M1/μ2 determines *in vitro* differences

* This work was supported in part by National Institutes of Health Public Health Service Grants R01 AI47904 (to M. L. N.) and K08 AI52209 (to J. S. L. P.) and by a Harvard Foundation-Giovanni Armenise Junior Faculty Research Grant (to M. L. N.). The costs of publication of this article were defrayed in part by the payment of page charges. This article must therefore be hereby marked "*advertisement*" in accordance with 18 U.S.C. Section 1734 solely to indicate this fact.

¶ Present address: James A. Baker Institute for Animal Health, College of Veterinary Medicine, Cornell University, Ithaca, NY 14853.

‖ To whom correspondence should be addressed: Dept. of Microbiology and Molecular Genetics, 200 Longwood Ave., Boston, MA 02115. Tel.: 617-645-3680; Fax: 617-738-7664; E-mail: mnibert@hms.harvard.edu.

[1] The abbreviations used are: mORV, mammalian *Orthoreovirus*; RTPase, RNA 5′-triphosphatase; NTPase, nucleoside triphosphatase; T1L, type 1 Lang; T3D, type 3 Dearing; wt, wild type; Sf21 cells, *S. frugiperda* 21 cells; A_{655}, absorbance at 655 nm; MES, 2-(*N*-morpholino)-ethanesulfonic acid.

TABLE I
mORV core proteins and their enzymatic activities

Core protein	Mass[a]	Copy no.[b]	Crystal structure	Enzymatic activities[c]	References
	kDa				
λ1	142	120	Yes[d]	NTPase	30
				RTPase	12
				RNA/DNA helicase	30
λ2	144	60	Yes[d]	RNA guanylyltransferase	14, 15, 17, 18
				RNA ^{7}N-methyltransferase	4, 16
				RNA $^{2'}O$-methyltransferase	4, 16
λ3	142	10–12	Yes[e]	RNA-dependent RNA polymerase	8, 9
μ2	83	20–24	No	NTPase	This study
				RTPase	This study
σ2	47	150	Yes[d]	None	

[a] Molecular mass from deduced sequence.
[b] Molecules per virion or core particle.
[c] Demonstrated *in vitro* or inferred from crystal structure in the cited references.
[d] Ref. 4.
[e] Ref. 9.

between T1L and T3D cores in both the response of the ATPase activities to temperature and the rate of GTP hydrolysis at certain conditions. The latter genetic associations are consistent with μ2 functioning as an NTPase or playing a regulatory role in the NTPase function of another core protein, most likely λ1 (23, 24, 30). Both μ2 and λ1 *in vitro* have also been shown to bind RNA (32–34). Thus, questions remain about the relative roles of μ2 and λ1 in the NTPase activities of cores and the specific roles each plays in viral mRNA synthesis.

Recent studies have used immunofluorescence microscopy to identify *in vivo* associations between μ2 and other proteins. Initially, μ2 was shown to associate with and stabilize microtubules in both infected and transfected cells (35). Subsequently, μ2 was shown to associate also with the major mORV nonstructural protein μNS (36). These findings suggest important roles for μ2 and μNS in building the cytoplasmic "factories" in which viral genome replication and assembly are thought to occur (35–38).

To learn more about the activities of μ2, we devised a purification protocol and undertook functional studies of the purified protein. Results in this report provide biochemical and genetic evidence that μ2 is itself a divalent cation-dependent NTPase and RTPase. Alanine substitutions in a putative nucleotide binding region of μ2 abrogated both functions but did not substantially affect the purification profile of the protein or its known associations with microtubules and μNS protein *in vivo*. *In vitro* microtubule binding by purified μ2 was also demonstrated and not affected by the mutations. Purified μ2 was further demonstrated to interact *in vitro* with the viral polymerase, λ3, and the presence of λ3 mildly stimulated the triphosphatase activities of μ2. These findings suggest that μ2 is an enzymatic component of the mORV core and may contribute several possible functions to viral mRNA synthesis.

EXPERIMENTAL PROCEDURES

Generation of a Recombinant Baculovirus for Expression of Wild-type (wt) μ2—Generation of plasmid pBS-M1(T1L), encoding wt T1L μ2 protein, was previously described (35). The complete μ2-encoding region was excised from this plasmid by digestion with BamHI and HindIII and ligated into the pFastBac vector (Invitrogen) under transcriptional control of the baculovirus (*Autographa californica* nuclear polyhedrosis virus) polyhedrin promoter. The resulting plasmid pFB-M1(T1L) was used to generate a recombinant baculovirus with the Bac-to-Bac system (Invitrogen). This baculovirus was amplified into high titer stocks by serial passage in *Spodoptera frugiperda* 21 cells (Sf21 cells).

Generation of a Recombinant Baculovirus for Expression of Mutant K415A/K419A μ2—To obtain an M1 gene encoding alanine substitutions for lysines 415 and 419 in μ2, we first removed the BamHI site from the multiple-cloning region of pBS-M1(T1L) by cutting with BamHI, filling the overhangs with Klenow polymerase, and religating. The resulting plasmid pBS′-M1(T1L) was used as template in an inverse polymerase chain reaction with forward primer 5′-GGGGATCCTTT***GC***ATCAACAATTATGAGAGTTC-3′ and reverse primer 5′-GGGGATCC***GC***AGGCAGCACAGCGCC-3′ (bold italics indicate nucleotide changes for Ala-419 and Ala-415, respectively). In each primer one silent nucleotide change was also introduced to generate a BamHI site (underlined) without affecting the μ2 amino acid sequence. The amplification conditions were the same as those described in Kim *et al.* (39). The resulting plasmid was subjected to nucleotide sequencing to confirm that between the BsmI and SphI sites in M1, and the BsmI-SphI fragment was then swapped for the same region of pBS-M1(T1L). The XbaI-HindIII fragment from the resulting plasmid pBS-M1(T1L)K415A/K419A was swapped for the same region of pFB-M1(T1L). The resulting plasmid pFB-M1(T1L)K415A/K419A was used to generate a recombinant baculovirus as indicated in the preceding section.

Cloning M1 Genes into the pCI-neo Vector—Generation of plasmid pCI-M1(T1L), encoding wt T1L μ2 protein, was previously described (35). The plasmid pCI-M1(T1L)K415A/K419A was generated in the same manner in that the M1 gene from pBS-M1(T1L)K415A/K419A was excised by digestion with SpeI and XhoI and ligated into the pCI-neo vector (Promega) that had been digested with NheI and SalI.

Purification of wt and K415A/K419A μ2—Sf21 cells were prepared in a 1-liter spinner at a concentration of 1×10^6 cells/ml, into which the recombinant baculovirus to express either wt or K415A/K419A μ2 was inoculated at 5–10 plaque-forming units/cell. At 60 h post-infection, the cells were harvested and washed 3 times with cold phosphate-buffered saline (137 mM NaCl, 3 mM KCl, 8 mM Na_2HPO_4, 1 mM KH_2PO_4, pH 7.5). Nuclear extracts were then prepared from these cells as follows. The cell pellet was washed twice with 50 ml of ice-cold Nonidet P-40 buffer and then twice with 50 ml of ice-cold $CaCl_2$ buffer. To make the Nonidet P-40 and $CaCl_2$ buffers 100 ml of Chelsky buffer (10 mM Tris, pH 7.0, 10 mM NaCl, 3 mM $MgCl_2$, 30 mM sucrose) was supplemented with Nonidet P-40 to 0.5% or $CaCl_2$ to 10 mM. The nuclear pellet was resuspended in 50 ml of lysis buffer (20 mM Tris, pH 7.9, 100 mM KCl, 0.2 mM EDTA, 20% glycerol, 1× protease inhibitor mixture (Roche Diagnostics)). Nuclei were lysed on ice with a syringe, and the nucleoplasm was separated from the postnuclear pellet by centrifugation at 15,000 rpm for 30 min in an RC-5B centrifuge with an SS34 rotor (DuPont Sorvall). The nucleoplasm was dialyzed overnight at 4 °C against A_0 buffer (20 mM Tris acetate, pH 8.5, 50 mM KCl, 5 mM $MgCl_2$, 10% glycerol, 2 mM β-mercaptoethanol).

All subsequent column work was performed at room temperature with an Akta-FPLC system (Amersham Biosciences). At each step the column fractions containing μ2 were identified by SDS-polyacrylamide gel electrophoresis and immunoblotting with μ2-specific polyclonal antiserum (36) and an alkaline phosphatase-based color detection method (39). The dialyzed nucleoplasm was applied to a 5-ml HiTrap DEAE-Sepharose column (Amersham Biosciences) preequilibrated with A_0 buffer. μ2 was eluted from this column at ~100 mM NaCl in a 0–1 M NaCl gradient in A_0 buffer as identified. The fractions containing μ2 were pooled, mixed 1:1 with A_0 buffer, and applied to a 1-ml HiTrap Blue (Cibacron Blue)-agarose column (Amersham Biosciences) preequilibrated with A_{50} buffer (A_0 buffer supplemented with 50 mM NaCl). μ2 eluted from this column at 0.8–1.2 M NaCl in a 0–2 M NaCl gradient in A_0 buffer. The fractions containing μ2 were pooled, dialyzed over-

night at 4 °C against A_0 buffer, and applied to a 1-ml HiTrap heparin-Sepharose column (Amersham Biosciences) preequilibrated with A_{50} buffer. μ2 eluted from this column at ~200 mM NaCl in a 0–1 M NaCl gradient in A_0 buffer. The fractions containing μ2 were pooled, dialyzed against A_{100} buffer (A_0 buffer supplemented with 100 mM NaCl), and used for all subsequent work as purified μ2. Protein concentration was estimated from absorbance at 280 nm. Yields from this procedure were routinely in the range of 300–400 μg of μ2 per 4×10^8 cells.

Purification of wt λ3 Protein—The T3D λ3 protein was expressed and purified as previously described (9). Immediately before use in each experiment, λ3 (or bovine serum albumin used in parallel samples) was dialyzed against A_{100} buffer for 2 h at 4 °C using a Slide-A-Lyzer 10K cassette (Pierce).

NTPase Assays—Reactions for analysis in the colorimetric NTPase assay were performed in A_{100} buffer lacking β-mercaptoethanol. The reactions also contained 2 mM ATP and the indicated amount(s) of protein(s) in a total reaction volume of 60 μl. For some experiments ingredients were altered as specifically described in the figure legends. After incubation at room temperature for an appropriate time (standard, 45 min), the reaction was stopped with 60 μl of 10% trichloroacetic acid. 100 μl of the stopped reaction was then mixed with 100 μl of colorimetric reagent prepared by mixing 6 N sulfuric acid, 0.8% ammonium molybdate, and 10% ascorbic acid in a 1:3:1 ratio. This mixture was incubated at 37 °C for 30 min, and absorbance at 655 nm (A_{655}) was measured with a microplate colorimeter (Molecular Devices). Standard curves generated with a dilution series of KH_2PO_4 were used to convert the A_{655} values to amounts of inorganic phosphate (P_i) released (23).

For the radiographic NTPase assay reaction conditions were the same as for the colorimetric assay except that the reaction volume was only 20 μl, and 5 μCi of [α-^{32}P]ATP (3000 Ci/mmol) (PerkinElmer Life Sciences) was used instead of 2 mM ATP. After incubating at room temperature for 30 min, the reaction was stopped with 10 mM EDTA. 1 μl of the stopped reaction was spotted onto a polyethyleneimine-cellulose thin-layer chromatography (TLC) plate (EM Science). After drying the TLC plate was developed in 1.2 M LiCl solvent, and the separated reaction products were visualized by either phosphorimaging (Molecular Dynamics) or exposure to x-ray film (Fuji or Kodak) in the presence of an intensifying screen.

RTPase Assay—MAXIscript *in vitro* transcription kit (Ambion) was used to generate γ-labeled 45-nucleotide RNA substrates following the manufacturer's directions. Each 20-μl reaction mixture contained 30 units of T7 RNA polymerase (from the kit), 1× transcription buffer (from the kit), 1 mM ATP, 1 mM CTP, 1 mM UTP, 0.03 mM GTP, 50 μCi of either [γ-^{32}P]GTP (6000 Ci/mmol) or [α-^{32}P]GTP (3000 Ci/mmol) (PerkinElmer), 1 μg of pGEM-4Z (Promega) (linearized with SmaI and purified from an agarose gel), and 1 unit/μl RNasin (Promega). After a 2-h incubation at 37 °C the reaction was adjusted to 50 μl with H_2O. Template DNA was degraded by treatment for 30 min at 37 °C with 2 units of DNase I (from the kit). Free nucleotides were removed with a nucleotide removal kit (Qiagen) and then a Sephadex G-25 column (Amersham Biosciences). The quality and purity of the purified 45-mer [γ-^{32}P]- or [α-^{32}P]RNA (*i.e.* appropriate RNA size and essential absence of [γ-^{32}P]- or [α-^{32}P]RNA and small abortive transcripts) were verified on 10% polyacrylamide gels containing 7 M urea (data not shown). Efficient removal of GTP and small abortive transcripts from the [γ-^{32}P]RNA was also verified by TLC, in which [γ-^{32}P]GTP was found to migrate slightly faster than the upper spot of the radiolabeled RNA (data not shown). RNA concentration was estimated by absorbance at 260 nm.

For the RTPase assay reaction conditions were the same as for the radiographic NTPase assay except that specified amounts of ^{32}P-labeled RNA were added instead of ATP. After incubating for the appropriate time at room temperature (standard, 1 h), the reaction was stopped with 10 mM EDTA. For Fig. 6, RNAs were resolved on a 10% polyacrylamide gel containing 7 M urea and then visualized by exposure to x-ray film in the presence of an intensifying screen. Otherwise, reaction products were separated by TLC as described for the radiographic NTPase assay and visualized by phosphorimaging. For quantitation from TLC, the intensity of the $^{32}P_i$ spot obtained in each μ2- and/or λ3-containing sample was expressed as a fraction of that obtained by treatment of the RNA with calf intestinal phosphatase (New England Biolabs). The upper spot attributable to substrate RNA in the TLC plates (see Fig. 7, *A* and *C*, for results with [γ-^{32}P]RNA substrate) was unexpected, suggesting that despite the purification steps and tests of purity described in the preceding section, the samples might be contaminated with GTP. However, the [α-^{32}P]RNA substrate was identically resolved into two spots by TLC, the upper of which was not abolished by prior treatment of the sample with calf intestinal phosphatase (data not shown), demonstrating that the upper spot is indeed attributable to RNA, not GTP.

Microtubule Spin-down Assay—A spin-down kit (Cytoskeleton, Inc.) was used according to the manufacturer's suggestions. Briefly, the indicated amounts of purified wt or K415A/K419A μ2 were mixed with microtubules stabilized with 20 μM taxol after polymerizing purified α- and β-tubulin by incubation at 37 °C for 20 min. After 40 min at room temperature, the mixtures were overlaid on a 100-μl sucrose cushion and spun at 100,000 × *g* for 40 min at room temperature in a TL-100 tabletop ultracentrifuge with a TLA-100 rotor (Beckman). The supernatant was removed, and the pellet was resuspended in 50 μl of phosphate-buffered saline. 10 μl of the resuspended pellet was then separated by SDS-polyacrylamide gel electrophoresis and analyzed by immunoblotting with μ2-specific polyclonal antiserum (36) and a horseradish peroxidase-based enhanced chemiluminescence detection method (Pierce).

Immunofluorescence Microscopy—Transfection was performed using 2 μg of plasmid DNA and 6 μl of LipofectAMINE reagent (Invitrogen) as previously described (35). At 18 h post-transfection cells were fixed with 100% methanol and stained with either Oregon Green-conjugated μ2-specific polyclonal antibodies, Texas Red-conjugated μNS-specific polyclonal antibodies, or both, as previously described (36). Fluorescence was visualized with a TE-300 inverted light microscope (Nikon), and the collected images were processed and optimized with Photoshop software (Adobe Systems).

Immunoprecipitation—Each of the indicated amounts of purified wt or K415A/K419A μ2 was mixed with 300 ng of purified λ3 in binding buffer (20 mM Tris, pH 8.5, 50 mM NaCl, 50 mM KCl, 5 mM $MgCl_2$, 10% glycerol, 0.01% Triton X-100, 2 mM β-mercaptoethanol, 1× protease inhibitor mixture). The mixtures were incubated overnight with rocking at 4 °C. μ2-specific polyclonal antibodies (purified from antiserum using a protein A column (36)) were added to a final concentration of 33 μg/ml, and the mixtures were incubated for an additional 2 h at 4 °C. Each mixture was supplemented with 10 μl of protein A Dynabeads (Dynal Biotech) preequilibrated with binding buffer and then incubated for 30 min at room temperature. Bead-bound antigen-antibody complexes were isolated with the use of a magnetic stand (Dynal Biotech) and washed twice with binding buffer and twice with washing buffer (binding buffer supplemented with NaCl to 200 mM and Triton X-100 to 0.05%). The washed beads were resuspended in 50 μl of 1× gel sample buffer (125 mM Tris, pH 8.0, 1% SDS, 2% β-mercaptoethanol, 10% sucrose, 0.01% bromphenol blue), boiled, separated by SDS-polyacrylamide gel electrophoresis, and analyzed by immunoblotting with either μ2- or λ3-specific polyclonal antiserum (36, 40) and an alkaline phosphatase-based color detection method (39).

RESULTS

Purification of mORV μ2 Protein—A protocol for large scale purification of μ2 protein has not been previously reported, and we, therefore, set out to devise one. Recombinant μ2 was expressed in Sf21 cells using a baculovirus vector in which the M1 gene was under control of the polyhedrin promoter. About half of μ2 expressed in this way appeared in the nuclear fraction of lysed cells (data not shown). This was not wholly unexpected since some nuclear localization of recombinant μ2 has been previously noted in mammalian cells by immunofluorescence microscopy (35, 36, 38), although the basis of this localization has remained unclear. The nucleoplasm (postnuclear supernatant) of μ2-expressing Sf21 cells was obtained and found to contain larger amounts of μ2 relative to other proteins than did the cytoplasm. The nucleoplasm was, therefore, used for further purification of μ2 on a series of ion-exchange and affinity columns: DEAE, Cibacron Blue, and heparin. SDS-polyacrylamide gel electrophoresis and immunoblotting with μ2-specific polyclonal antiserum were used to identify the column fractions containing μ2. Fig. 1*A* summarizes representative gel results from the series and shows that one major protein band ($M_r \sim 80{,}000$) was strongly enriched. This band comigrated with the μ2 protein from mORV cores during electrophoresis (Fig. 1*B*, *left*) and was also recognized by the μ2 antiserum in immunoblots (Fig. 1*B*, *right*). Another band sometimes seen migrating above μ2 (Fig. 1, *B*, *left*, and *C*) was a contaminant found in different amounts in different prepara-

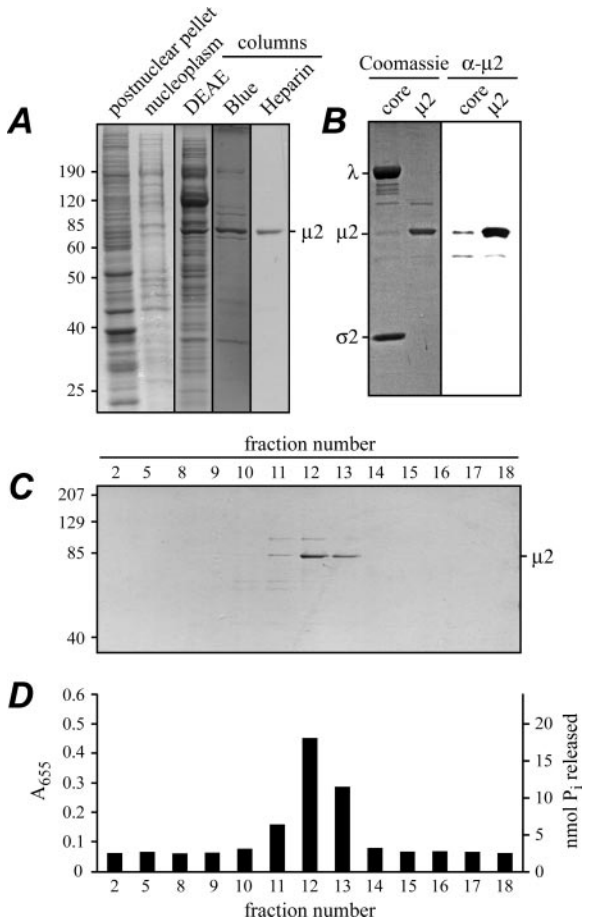

FIG. 1. **Purification of mORV μ2 protein and analysis of its ATPase activity.** Denatured proteins were resolved by electrophoresis on SDS-polyacrylamide mini-gels (10% acrylamide), which were then either stained with Coomassie Brilliant Blue R-250 or electroblotted as indicated. *A*, mORV μ2 protein was obtained from the nucleoplasm of Sf21 cells and progressively purified over DEAE, Cibacron Blue, and heparin columns. Aliquots from the postnuclear pellet, the nucleoplasm, and the peak fractions from each column were evaluated in stained gels. Positions of size markers (kDa) (Invitrogen) are indicated at the *left*. *B*, samples of purified mORV cores and purified μ2 protein were evaluated in adjacent lanes of a stained gel (*left*). An identical gel was prepared for immunoblot analysis with μ2-specific polyclonal antiserum (*right*). *C*, aliquots of numbered fractions from the heparin column were evaluated in adjacent lanes of a stained gel. Positions of size markers (kDa) (Bio-Rad) are indicated at left. *D*, all fractions shown in *C* were analyzed for their capacity to release P_i from ATP as measured by A_{655} in a colorimetric assay.

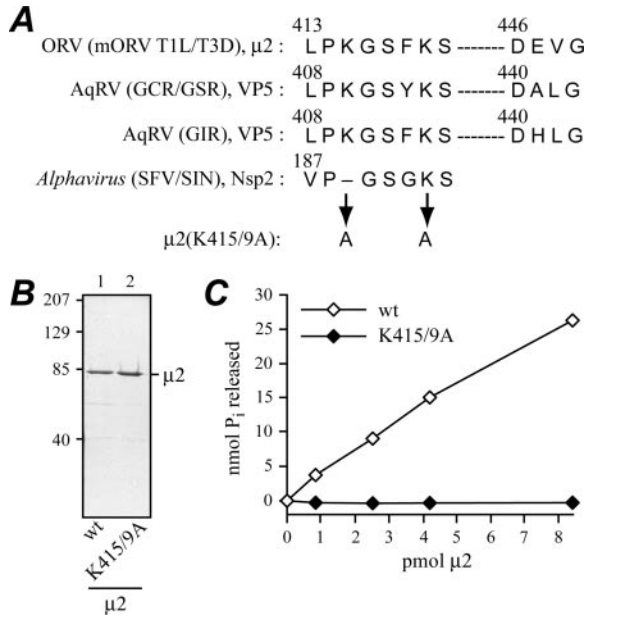

FIG. 2. **Evidence for involvement of μ2 residues 415 and/or 419 in ATP hydrolysis.** *A*, putative nucleotide binding motifs in the *Orthoreovirus* (*ORV*) μ2 and *Aquareovirus* (*AqRV*) VP5 proteins. Specifically shown are sequences of mORV T1L and T3D μ2 (35, 55, 56), grass carp and golden shiner reovirus (*GCR/GSR*) VP5 (41), and golden ide reovirus (*GIR*) VP5 (41). Conserved sequences from *Alphavirus* (*e.g.* Semliki Forest virus (*SFV*) and Sindbis virus (*SIN*)) Nsp2, a known NTPase and RTPase (28, 42), are also shown. Amino acid position numbers are indicated *atop* each sequence. Positions of alanine-for-lysine substitutions in μ2 mutant K415A/K419A (*K415/9A*) are also indicated. *B*, denatured samples of the purified wt and K415A/K419A μ2 proteins were resolved in adjacent lanes of an SDS-polyacrylamide mini-gel (10% acrylamide), which was then stained with Coomassie Brilliant Blue R-250. Positions of size markers (kDa) (Bio-Rad) are indicated at the *left*. *C*, P_i released from ATP was measured by A_{655} in a colorimetric assay. Samples containing wt or K415A/K419A μ2 were analyzed in parallel.

tions; it was not recognized by the μ2 antiserum. A minor band migrating below μ2 (M_r 50,000–60,000) but recognized by the μ2 antiserum was seen in samples of both cores and purified protein (Fig. 1*B*), suggesting it is a common degradation product of μ2. Preliminary evidence from dynamic light scattering and gel filtration chromatography suggested the purified form of μ2 is most likely a dimer.[2] We also found that μ2 expressed from this same baculovirus vector was competent to be packaged into core-like particles when coexpressed with other core proteins.[3]

NTP Hydrolysis by Purified μ2 Protein—To determine whether purified μ2 has ATPase activity we examined aliquots of the heparin-column fractions with a colorimetric assay that detects the P_i released by ATP hydrolysis (23, 24). Fig. 1, *C* and *D*, show results of a representative experiment. The assay revealed that fraction numbers 11–13 in this experiment had a level of ATPase activity substantially above the background level of other fractions (Fig. 1*D*). These same fractions were shown to contain the highest amounts of μ2 protein by gel analysis (Fig. 1*C*). Moreover, the level of ATPase activity of each fraction was proportional to the amount of μ2 the fraction contained (fraction 12 > 13 > 11), strongly suggesting that μ2 is required for the activity. Other colorimetric assays with the peak fractions provided evidence that μ2 is able to hydrolyze GTP, CTP, and UTP as less preferred substrates (data not shown), suggesting that μ2 is a nonspecific NTPase.

Mutant μ2 Protein (K415A/K419A) with Alanine Substitutions in a Putative Nucleotide Binding Motif—After the preceding results we remained concerned that the NTPase activity might be attributable to a contaminant and not μ2 in the purified preparation. To prove that NTP hydrolysis was mediated by μ2 we sought to create a μ2 mutant that lacked this activity. We have previously noted a conserved region of the μ2 primary sequence with some similarities to nucleotide binding A and B motifs (24) (Fig. 2*A*). Comparison with recently reported sequences for the homologous VP5 proteins of *Aquareovirus* (41) showed these motifs are conserved despite an overall μ2-VP5 homology of only 24%[4] (Fig. 2*A*). Moreover, the putative A motif of *Ortho-* and *Aquareovirus* is very similar to that of *Alphavirus* Nsp2, a known NTPase and RTPase (28, 42) (Fig. 2*A*). We, therefore, introduced two alanine-for-lysine substitu-

[2] X. Lu, J. Kim, M. L. Nibert, and S. C. Harrison, unpublished observation.

[3] J. Kim and M. L. Nibert, unpublished observation.

[4] J. Kim, Y. Tao, K. M. Reinisch, S. C. Harrison, and M. L. Nibert, submitted for publication.

tions at positions 415 and 419 in the putative A motif (Fig. 2*A*) in an effort to eliminate the apparent NTPase activity of μ2.

The μ2 mutant K415A/K419A was expressed using a baculovirus vector and purified through the same procedures as wt μ2. Gels showed no mobility difference between the purified K415A/K419A and wt proteins (Fig. 2*B*; data not shown). Over the series of columns in the purification, the mutant behaved almost identically to wt protein, except that K415A/K419A μ2 was eluted at slightly lower salt concentration from the Cibacron Blue column (data not shown). The similar purification patterns suggest the mutant is folded and structurally similar to wt protein (see Fig. 3 and "Microtubule Binding and μNS Association by wt and K415A/K419A μ2" below for more evidence). The colorimetric assay revealed that the ATPase activity of purified wt μ2 increased in concert with protein concentration, whereas the activity of K415A/K419A μ2 remained at background level across the range of concentrations (Fig. 2*C*). These results indicate that μ2 is itself an ATPase and suggest that its putative nucleotide binding A motif is involved in this activity. Based on the comparison with *Alphavirus* Nsp2 (Fig. 2*A*), we consider it likely that the conserved Lys-419 residue in mORV μ2 is especially important. It is also interesting that the proline residue conserved in *Ortho/Aquareovirus* μ2/VP5 and *Alphavirus* Nsp2 is one of two residues mutated in the temperature-sensitive μ2 protein of mORV mutant *tsH11.2* (43).

Microtubule Binding and μNS Association by wt and K415A/K419A μ2—The preceding results with the K415A/K419A mutant would be most convincing if the effect were limited to NTP hydrolysis, whereas other activities of μ2 are spared. Such findings would indicate that the K415A/K419A mutations do not globally disrupt the folding and structure of μ2. The fact that K415A/K419A μ2 could be purified in a similar manner to wt μ2 provided some evidence in this regard, but we sought further evidence. Recent work from our laboratory has shown the capacity of μ2 to associate with both microtubules and mORV μNS protein in infected and transfected cells (35, 36). We, therefore, tested the mutant for these activities. In transfected CV-1 cells, K415A/K419A μ2 associated with microtubules similarly to wt μ2 (Fig. 3*A*). A substantial portion of both μ2 proteins localized to the nucleus (Fig. 3*A*), as previously noted for wt μ2 (35, 36). The exact role if any of this nuclear localization remains unknown. To complement the *in vivo* results demonstrating association between μ2 and microtubules, we performed an *in vitro* spin-down assay with a mixture containing taxol-stabilized microtubules (44, 45) and increasing concentrations of either wt or K415A/K419A μ2. After proteins in the pellets were separated on SDS-polyacrylamide gels, immunoblots revealed that the K415A/K419A mutant was spun down with microtubules as well as wt μ2, whereas neither was spun down in the absence of microtubules (Fig. 3*B*). These results provide strong evidence that μ2 binds directly to microtubules and also show that the K415A/K419A mutant has a microtubule binding capacity similar to that of wt protein. When transiently expressed in CV-1 cells, the μNS protein, a major component of viral factories in mORV-infected cells (36), formed globular inclusions within the cytoplasm (Fig. 3*C*, *bottom*), as previously reported (36). When wt μ2 was coexpressed with μNS, on the other hand, μNS localized to microtubules along with μ2 (Fig. 3*C*, *upper left*), as also previously reported (36). When K415A/K419A μ2 was coexpressed with μNS, μNS again localized to microtubules along with μ2 (Fig. 3*C*, *upper right*). In sum, these results demonstrate that K415A/K419A μ2 behaves like wt μ2 with regard to microtubule binding both *in vivo* and *in vitro*, nuclear localization, and interaction with μNS *in vivo*, indicating that the two forms of μ2 are functionally similar in many regards. We conclude that the K415A/K419A mutations have little or no effect on the overall conformation of μ2 but specifically abrogate its ATPase activity.

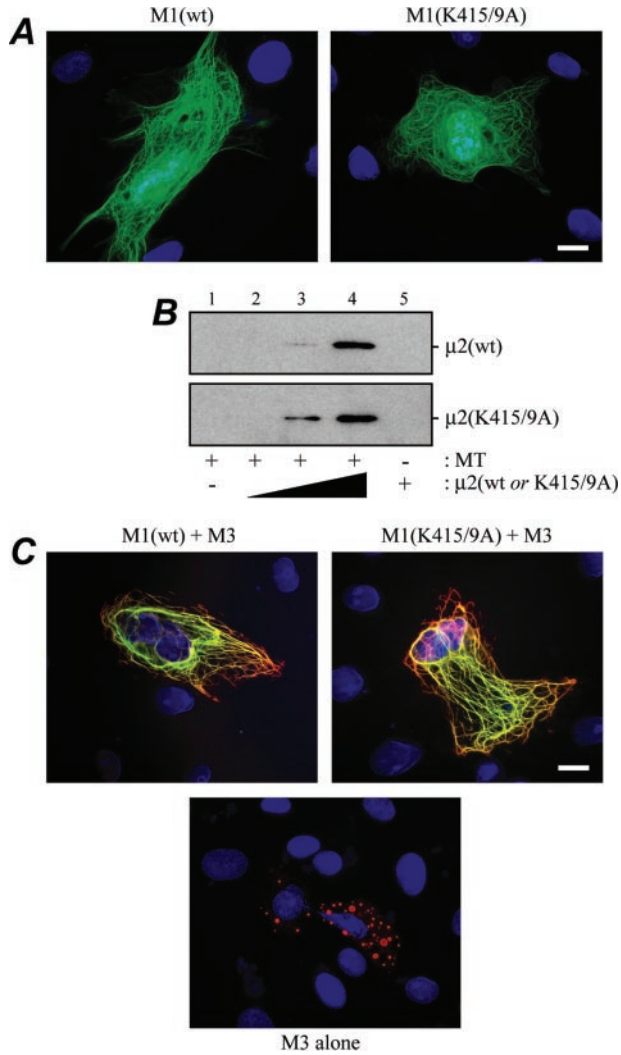

FIG. 3. **Associations of wt and K415A/K419A μ2 with microtubules and μNS.** Proteins in CV-1 cells were visualized by immunofluorescence microscopy. Cell nuclei were stained with 4,6-diamidino-2-phenylindole (*blue*). *Scale bars*, 10 μm. *A*, the wt or K415A/K419A (*K415/9A*) μ2 protein was expressed in cells transfected with pCI-neo plasmids containing the respective M1 genes. At 18 h post-transfection, cells were fixed, and μ2 was immunostained with Oregon Green-conjugated μ2-specific polyclonal antibodies (*green*). *B*, increasing amounts of purified wt μ2 (*top*) or K415A/K419A μ2 (*bottom*) (0, 0.84, 1.8, or 4.2 pmol each in *lanes 1–4*) were mixed with microtubules (*MT*) stabilized by taxol after tubulin polymerization *in vitro* and sedimented through a sucrose cushion. Control samples containing no microtubules (*lane 5*, 4.2 pmol of μ2) were also analyzed. Proteins in the sedimented pellets were resolved in adjacent lanes of an SDS-polyacrylamide mini-gel (10% acrylamide), which was then subjected to immunoblot analysis with μ2-specific polyclonal antiserum. *C*, the wt μ2, K415A/K419A μ2, and/or wt μNS proteins were expressed in cells transfected with pCI-neo plasmids containing the respective M1 or M3 genes. μNS was separately coexpressed with each μ2 protein (*top*) and was also expressed in the absence of μ2 (*bottom*). At 18 h post-transfection, cells were fixed, and μ2 and μNS were respectively immunostained with Oregon Green-conjugated μ2-pecific polyclonal antibodies (*green*) and Texas Red-conjugated μNS-specific polyclonal antibodies (*red*).

Specificity of wt μ2 for Release of γ-Phosphate from NTPs—The μ2- and λ1-influenced NTPase activities in mORV cores are specific for triphosphorylated nucleotides and release only the γ-phosphate (21–24, 30). We, therefore, tested for such specificity with the purified μ2 proteins. [α-^{32}P]ATP was used as substrate in a radiographic assay in which the reaction products were analyzed by TLC and fluorography. In this assay

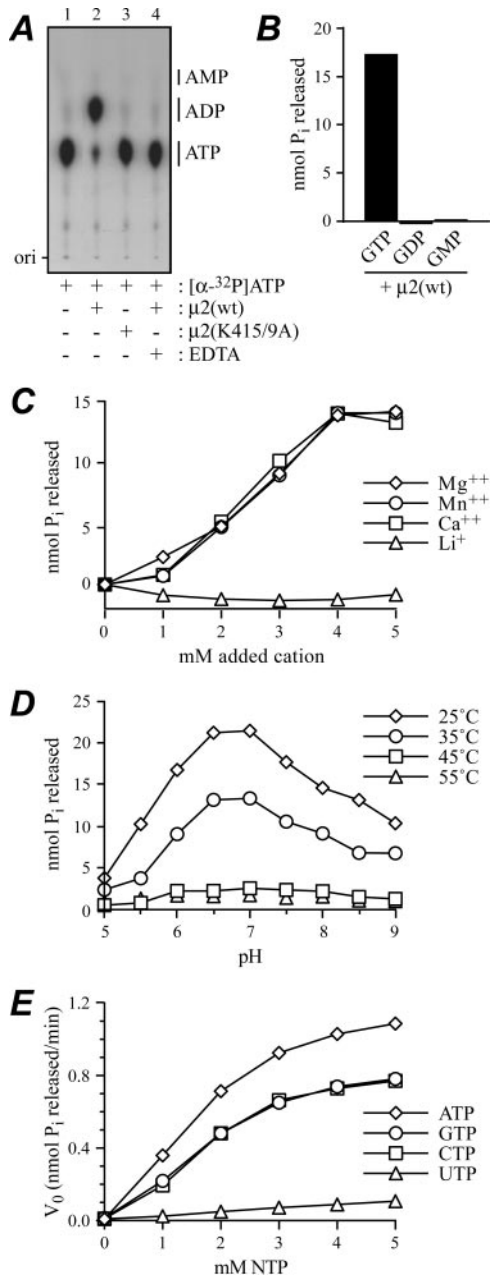

FIG. 4. **Characteristics of the NTPase activities of wt μ2.** Test samples contained 2.9 pmol of μ2 protein unless otherwise stated. *A*, the products of hydrolysis of [α-^{32}P]ATP by either wt μ2 (*lane 2*) or K415A/K419A (*K415/9A*) μ2 (*lane 3*) were separated by TLC and visualized by fluorography. Control samples containing either no μ2 (*lane 1*) or wt μ2 in the presence of 10 mM EDTA (*lane 4*) were also analyzed. *ori*, sample origins. *B*, guanosine nucleotides (2 mM GTP, GDP, or GMP) were tested for hydrolysis by wt μ2. Test samples contained 6.0 pmol of wt μ2. *C*, indicated concentrations of different cations (chloride salts) were tested for the effects on ATP hydrolysis by wt μ2. *D*, buffers at the indicated pH values were tested at different temperatures for effects on ATP hydrolysis by wt μ2. Each buffer was made as a 5× stock by mixing 100 mM Tris and 100 mM MES until the desired pH was reached. Other contents of the reaction mixtures were the same as in other experiments. *E*, the indicated concentrations of the different NTPs were tested for the effects on NTP hydrolysis by wt μ2. Initial velocities (V_0) were determined from time points within the linear range of each reaction time course. In *B–E*, P_i released from the nucleotide substrate was measured by A_{655} in a colorimetric assay.

wt μ2 generated ADP as the only radiolabeled product (Fig. 4*A*, *lane 2*), indicating that μ2 specifically attacks the β-γ phosphodiester linkage of ATP, generating ADP (labeled) and P_i (not labeled) as products. As expected from previous results,

TABLE II
Kinetic properties of NTPase and RTPase activities of mORV μ2 protein

Exp. no.	Substrate ± pmol of added λ3	V_{max} [a]	K_m [a]	K_{cat} [b]
		nmol or fmol min^{-1}	*mM or μM*	*min^{-1}*
1	ATP	2.4	2.5	830
2	ATP	1.7	2.9	590
2	GTP	1.4	3.7	480
2	CTP	1.3	3.8	440
2	UTP	0.29	9.4	73
3	ATP	0.93	2.5	320
3	ATP + 0.87	1.0	2.6	350
3	ATP + 4.4	1.3	2.6	450
4	RNA	36 fmol min^{-1}	0.32 μM	0.30

[a] Estimated from hyperbolic fits to the Michaelis-Menten equation by nonlinear regression with Prism 4.0 (GraphPad Software). V_{max} values are expressed in nmol min^{-1} unless otherwise indicated. K_m values are expressed in mM unless otherwise indicated. Differing V_{max} values for ATP hydrolysis between experiments reflect variation in the levels of activity observed with different purified preparations of wild-type μ2 and after different times of protein storage at 4 °C. K_m values for ATP hydrolysis were much less variable (2.6 ± 0.2 mM) in these experiments.
[b] Turnover number calculated from V_{max} and amount of wild-type μ2 in each reaction.

K415A/K419A μ2 showed no activity in this assay (Fig. 4*A*, *lane 3*). The addition of EDTA to the reaction containing wt μ2 completely abolished the ATPase activity (Fig. 4*A*, *lane 4*), indicating that the activity is dependent on divalent cations, as are many other NTPases (25–29) including those in mORV cores (23) (see below for additional evidence). Specific cleavage of the β-γ phosphodiester linkage was further indicated by experiments in which the colorimetric assay was used to examine the capacity of wt μ2 to hydrolyze GTP, GDP, or GMP and which showed that only GTP could serve for P_i release (Fig. 4*B*).

Other Characteristics of the NTPase Activities of wt μ2—NTPase activities are commonly sensitive to the type and concentration of divalent cations in the reaction mixture (25–29). We, therefore, tested the ATPase activity of μ2 in the presence of increasing concentrations of different cations. The results demonstrated that mM concentrations of a divalent cation are necessary for the activity and that Ca^{2+}, Mg^{2+}, or Mn^{2+} can each serve similarly well in this capacity (Fig. 4*C*). Synergistic effects of Mg^{2+} and Mn^{2+} (26) were not observed (data not shown). In other experiments we found that the pH optimum for ATP hydrolysis by μ2 was 6.5–7.0 (Fig. 4*D*). However, the activity remained high, above 50% of maximum, over a broad range of pH values between ~5.7 and >9.0 (Fig. 4*D*). At higher temperatures (45 or 55 °C) little activity was seen, and the activity at 25 °C was higher than that at 35 °C (Fig. 4*D*). Experiments to estimate the V_{max}, apparent K_m, and K_{cat} values of wt μ2 in hydrolysis of each NTP were performed with increasing concentrations of ATP, GTP, CTP, or UTP (Fig. 4*E*). The results confirmed ATP as the preferred substrate for hydrolysis and suggested this preference is based in modest increases in both substrate binding affinity and catalytic efficiency relative to GTP or CTP (Table II). UTP was a relatively poorer substrate for hydrolysis (Table II). These estimated values for the kinetic properties of μ2 in NTP hydrolysis are similar to published findings for several other viral NTPases (see "Discussion").

λ3 Interaction with wt and K415A/K419A μ2—The two stoichiometrically minor core proteins, μ2 and λ3, have been hypothesized to interact within cores (46–48). Direct evidence has remained lacking, but evidence from electron cryomicroscopy has suggested that the two proteins are at least juxtaposed in the core interior (5). In addition, the genetic evidence that μ2 can influence core transcriptase behaviors has sug-

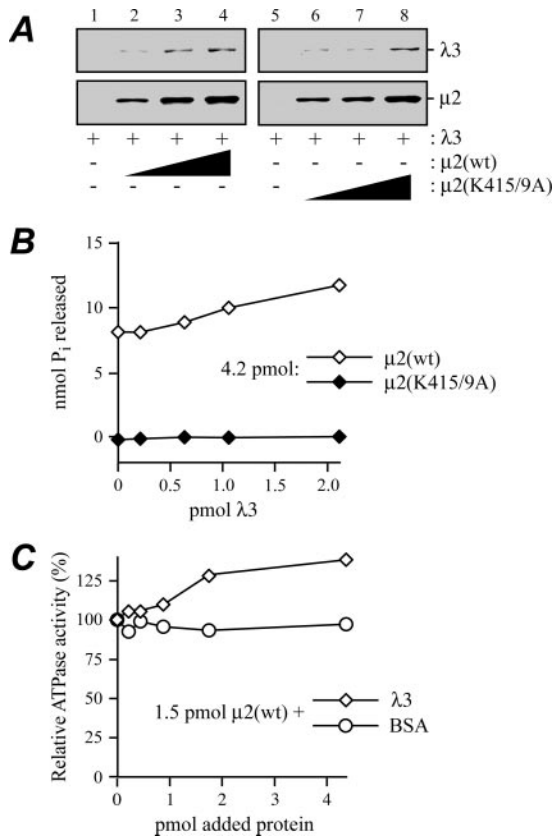

FIG. 5. **μ2-λ3 interaction and stimulation of μ2-mediated ATPase activity by λ3.** *A*, increasing amounts (0, 0.84, 1.8, or 4.2 pmol) of either wt μ2 (*lanes 1–4*) or K415A/K419A (*K415/9A*) μ2 (*lanes 5–8*) were mixed with 2.1 pmol of λ3 protein and subjected to immunoprecipitation using μ2-specific polyclonal antibodies. After extensive washing, the immunoprecipitates were resolved in adjacent lanes of an SDS-polyacrylamide mini-gel (10% acrylamide), which was then subjected to immunoblot analysis. Appropriate portions of the blot were probed with polyclonal antiserum specific for either λ3 (*top*) or μ2 (*bottom*). *B*, levels of ATP hydrolysis by 4.2 pmol of either wt or K415A/K419A μ2 were determined in parallel in the presence of increasing amounts (0, 0.21, 0.63, 1.1, or 2.1 pmol) of λ3. *C*, levels of ATP hydrolysis by 1.5 pmol of wt μ2 were determined in the presence of increasing amounts (0, 0.21, 0.44, 0.87, 1.7, or 4.4 pmol) of either λ3 or bovine serum albumin (*BSA*) in parallel. Activity values are expressed as a percentage relative to an average of those obtained in the absence of λ3 or bovine serum albumin. In *B* and *C* P_i released from ATP was measured by A_{655} in a colorimetric assay.

gested a μ2-λ3 interaction (31). A protocol is available for large scale purification of λ3 (8, 9) and was used in this study to obtain purified λ3 for investigating its possible interaction with purified μ2 *in vitro*. In the absence of μ2, λ3 was not immunoprecipitated by μ2-specific polyclonal antibodies (Fig. 5*A*, *lanes 1* and *5*). In the presence of increasing concentrations of either wt or K415A/K419A μ2, however, the amount of λ3 precipitated by the μ2 antibodies was progressively increased (Fig. 5*A*, *lanes 2–4* and *6–8*). These results indicate that μ2 can indeed interact with λ3 *in vitro*. They also indicate that the K415A/K419A mutations do not affect this interaction, providing further evidence for the largely intact conformation of this mutant μ2.

λ3 Stimulation of ATPase Activity of wt μ2—Having demonstrated μ2-λ3 interaction, we hypothesized that λ3 binding to μ2 may stimulate the enzymatic activities of the latter. In the colorimetric assay for ATPase activity, neither λ3 alone nor mixtures of K415A/K419A μ2 with increasing concentrations of λ3 showed activity (Fig. 5*B*). These findings suggested that λ3 does not have intrinsic ATPase activity (that is, in the presence of ATP but no other nucleoside triphosphates or template RNA)

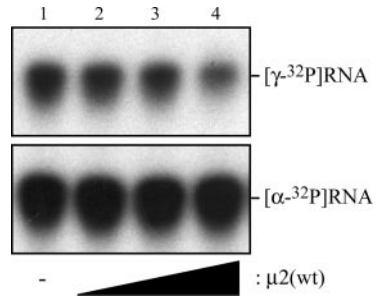

FIG. 6. **RTPase activity of wt μ2 examined by gel electrophoresis.** Loss of radiolabel from 45-mer RNA substrates, synthesized in the presence of [γ-^{32}P]GTP (*top*) or [α-^{32}P]GTP (*bottom*), was visualized by fluorography after resolution of the RNAs in a denaturing polyacrylamide gel (10%). Each test sample contained 0.4 μM substrate RNA and one of the following amounts of purified wt μ2 protein: 0 (*lane 1*), 0.024 (*lane 2*), 0.060 (*lane 3*), or 0.18 (*lane 4*) pmol.

and also that K415A/K419A μ2 could not be stimulated to demonstrate this activity by its interaction with λ3. On the other hand, mixtures of wt μ2 with increasing concentrations of λ3 exhibited increasing levels of ATPase activity (Fig. 5, *B* and *C*), suggesting that μ2-λ3 interaction mildly stimulated this activity of wt μ2. Increasing concentrations of bovine serum albumin had no effect on the ATPase activity of wt μ2 (Fig. 5*C*), providing evidence that the stimulatory effect was specific to λ3. An experiment to estimate the effects of λ3 on the kinetic properties of μ2 in ATP hydrolysis (data not shown) suggested that increasing amounts of λ3 progressively increased the K_{cat} of the reaction but had little effect on its apparent K_m (Table II). This last finding suggests that λ3 acted to increase the catalytic efficiency of μ2 and not its substrate binding affinity.

RTPase Activity of wt μ2—The capacity of wt μ2 to release the γ-phosphate from an NTP led us to hypothesize that μ2 may also release the 5′ γ-phosphate from an RNA molecule. mORV cores mediate such an RTPase activity, which yields a diphosphorylated RNA 5′ end (11, 49) for linkage to GMP by the λ2-associated guanylyltransferase (4, 11, 14, 15, 17, 18), as part of the mRNA capping process. The RTPase activity has been previously attributed to the λ1 shell protein (12). We nevertheless considered it possible that this activity may instead be represented by the NTPase activity of μ2, and we, therefore, tested purified μ2 for its capacity to release the γ-phosphate from RNA. An *in vitro* transcription reaction driven by T7 RNA polymerase was performed in the presence of [γ-^{32}P]GTP to generate RNA transcripts 45 nucleotides in length in which only the 5′-terminal γ-phosphate was radiolabeled. Alternatively, the reaction was performed in the presence of [α-^{32}P]GTP to generate 45-mer transcripts with the radiolabel in internal positions. The quality of these substrate RNAs and their essential lack of contamination with [γ-^{32}P]- or [α-^{32}P]RNA were confirmed by electrophoresis in denaturing polyacrylamide gels (data not shown). After incubation in the presence of purified wt μ2 followed by denaturing gel analysis, loss of radiolabel from the 45-mer RNA was observed with the [γ-^{32}P]GTP-labeled substrate but not the [α-^{32}P]GTP-labeled substrate (Fig. 6). These results indicate that μ2 indeed displays RTPase activity and not a nonspecific nuclease activity that would have degraded both substrates.

The RTPase activity of μ2 was further analyzed by TLC. This assay revealed that wt μ2 in the presence of increasing concentrations of [γ-^{32}P]GTP-labeled substrate RNA released increasing amounts of ^{32}P-labeled P_i (Fig. 7*A*, *lanes 3–7*). The addition of EDTA abolished the γ-phosphate release from RNA by wt μ2 (Fig. 7*A*, *lane 8*), indicating that the RTPase activity is dependent on divalent cations, as is the NTPase activity. K415A/K419A μ2 showed no activity in the RTPase assay (Fig. 7*A*,

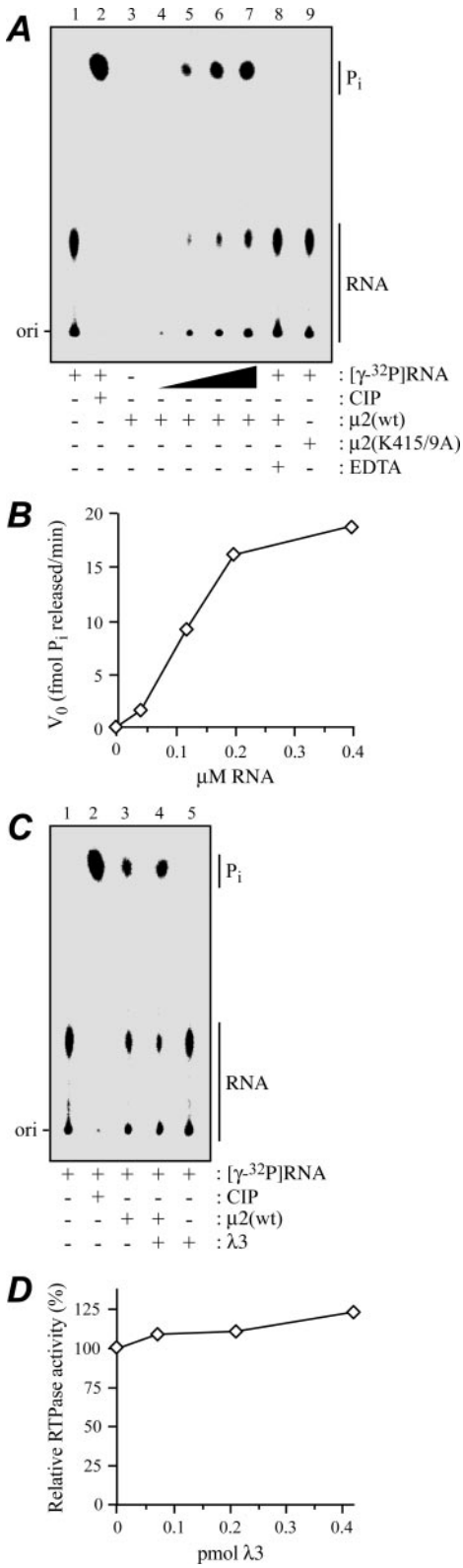

FIG. 7. **RTPase activity of wt μ2 examined by TLC and stimulation by λ3.** Release of ^{32}P-labeled P_i from [γ-^{32}P]GTP-labeled 45-mer RNA was visualized by phosphorimaging after separation of reaction products by TLC. Test samples contained 0.12 pmol of μ2 protein unless otherwise stated. *A*, levels of RTPase activity by wt μ2 were determined in the presence of increasing concentrations of substrate RNA (0, 0.04, 0.12, 0.2, or 0.4 μM) (*lanes 3–7*). Control samples containing no μ2 (*lane 1*), wt μ2 in the presence of 10 mM EDTA (*lane 8*), or K415A/K419A (*K415/9A*) μ2 (*lane 9*), each with 0.4 μM substrate RNA, were also analyzed. A control sample containing 0.4 μM substrate RNA and 3 units of calf intestinal phosphatase (*CIP*) (*lane 2*) was included to demonstrate complete release of the ^{32}P-labeled γ-phosphate. *ori*, sample origins. *B*, indicated concentrations of substrate RNA were tested for effects on the RTPase activity of wt μ2. Initial velocities (V_0) were determined from time points within the linear range of each reaction time course. *C*, levels of RTPase activity by wt μ2 were determined in the presence of 0.4 μM substrate RNA and either 0 or 0.42 pmol of λ3 protein (*lanes 3* and *4*). Control samples containing no μ2 or λ3 (*lane 1*) or 0.42 pmol of λ3 but no μ2 (*lane 5*), each with 0.4 μM substrate RNA, were also analyzed. A calf intestinal phosphatase control was included as in *panel B* (*lane 2*). *D*, levels of RTPase activity by wt μ2 were determined in the presence of increasing amounts of λ3 (0, 0.07, 0.21, or 0.42 pmol). Activity values are expressed as a percentage of that obtained in the absence of λ3. Some substrate RNA remained at the sample origins in these experiments, as seen in *A* and *C*.

lane 9). This last result suggests that the RTPase activity involves the same putative nucleotide binding region of μ2 as the NTPase, since the K415A/K419A mutations abolished both activities. Consistent with the release of γ-phosphate by wt μ2, the amount of uncleaved RNA substrate was decreased relative to that in the RNA-alone, EDTA, or K415A/K419A μ2 lane (Fig. 7*A*, compare *lane 7* with *lanes 1*, *8*, or *9*). The decreased amount of uncleaved [γ-^{32}P]RNA substrate, after incubation with wt μ2, was confirmed by electrophoresis in a denaturing 10% polyacrylamide gel, as was the failure of wt μ2 to degrade [α-^{32}P]RNA (data not shown). An experiment to estimate the kinetic properties of μ2 in the RTPase reaction (Fig. 7*B*) suggested that its V_{max}, apparent K_m, and K_{cat} values were all substantially lower than those for NTP hydrolysis (Table II). This is consistent with published findings for other viral proteins having both NTPase and RTPase activities (see "Discussion").

λ3 Stimulation of RTPase Activity of wt μ2—Preceding evidence for the capacity of λ3 to stimulate the ATPase activity of wt μ2 (Fig. 5, *B* and *C*) led us to expect a similar effect on RTPase activity. Indeed, when [γ-^{32}P]RNA was used as substrate neither λ3 alone (Fig. 7*C*, *lane 5*) nor mixtures of K415A/K419A μ2 with λ3 (data not shown) exhibited RTPase activity, but mixtures of wt μ2 with increasing concentrations of λ3 exhibited mildly increasing levels of RTPase activity (Fig. 7*C*, *lanes 3* and *4*; Fig. 7*D*). These findings suggest that λ3 does not have intrinsic RTPase activity, that K415A/K419A μ2 cannot be stimulated to demonstrate RTPase activity by its interaction with λ3, and that the presence of λ3 mildly stimulates the RTPase activity of wt μ2.

DISCUSSION

Results in this report demonstrate that mORV μ2 protein in the presence of divalent cations can catalyze removal of the γ-phosphate from either an NTP or the 5′ end of an RNA. When a purified protein is shown to exhibit a new enzymatic activity, it is always possible that the activity is attributable to a contaminant in the preparation and not the protein of interest. To rule out that possibility we introduced alanine substitutions in μ2 that we expected to reduce its NTPase and/or RTPase activities because the substitutions were located in a putative nucleotide binding region of μ2. These substitutions did not substantially affect the purification profile of the protein but did abolish its capacity for γ-phosphate removal from either type of substrate. Thus, both activities are attributable to the wt μ2 protein. Moreover, both activities involve the same putative nucleotide binding region of μ2 in which the alanine substitutions were located. An asparagine substitution for Lys-192 in Semliki Forest virus (*Alphavirus*) Nsp2 (see Fig. 2*A*) has been shown to abrogate both its NTPase and its RTPase activities (28). Similarly, alanine substitutions that inactivate the baculovirus and vaccinia virus RTPases also abrogate their NTPase activities (25, 26, 29).

Further evidence that the NTPase and RTPase activities are

attributable to μ2 is that λ3 mildly stimulated both activities of wt but not mutant, μ2. A viral component such as λ3 would be unlikely to have a stimulatory effect on the activities of a cellular contaminant, but since λ3 interacts with μ2 (Fig. 5), its stimulatory effect on the NTPase and RTPase activities of μ2 is not surprising. Because (i) λ3 alone did not show these activities, (ii) no increase in activities was seen when λ3 was incubated with mutant μ2, and (iii) λ3 interacts with both wt and mutant μ2, the increase in activities when λ3 was incubated with wt μ2 cannot be attributed to an effect of μ2 binding on latent activities of λ3. The new evidence for μ2-λ3 interaction *in vitro* also supports the hypothesis that λ3 and μ2 interact within mORV cores, as previously suggested by electron cryomicroscopy and genetic results (5, 31). Such an interaction would further manifest the close juxtaposition of different transcription and capping enzymes through protein-protein contacts within viral particles (4, 5) (see Table I), as has been recently shown for analogous cellular enzymes (for review, see Ref. 50 and 51).

Our estimated values for the kinetic properties of μ2 in NTP hydrolysis (Table II) are similar to published ones for several other divalent cation-dependent viral NTPases. For example, the apparent K_m for ATP hydrolysis by NTPase/RNA helicase NPH-II from vaccinia virus has been reported as 1.2 mM (52), and the K_{cat} for ATP hydrolysis by NTPase/RTPase D1 from vaccinia virus has been reported as 606 min^{-1} (27). In addition, we found apparent K_m and K_{cat} values for the triphosphatase activities of μ2 to be much lower for RNA than for NTP substrates (Table II), and this trend has also been seen with other viral proteins. For example, the apparent K_m for the RTPase activity of vaccinia virus D1 has been reported as 1.0 μM compared with 0.8 mM for ATP hydrolysis (27), and the K_{cat} for the RTPase activity of Semliki Forest virus Nsp2 has been reported as 5.5 min^{-1}, compared with 230 min^{-1} for GTP hydrolysis (28).

The literature indicates that it is common for RTPases to exhibit NTPase activities (25–29). The reciprocal statement is harder to support, however, because NTPases have been less routinely tested for RTPase activity. We nonetheless expect that many NTPases could act as RTPases *in vitro* without the latter being a normal aspect of their functions in cells. Thus, our demonstration that μ2 exhibits RTPase activity *in vitro* does not necessarily mean that it acts as an RTPase in cores. The same logic applies to the *in vitro* RTPase activity reported for the mORV λ1 protein (12).

The findings in this report corroborate previous genetic evidence for a role of μ2 in mORV core NTPase activities (24). Future investigations can now be focused on the specific role(s) of the triphosphatase activities of μ2 in core functions. For example, it will be important to dissect whether μ2 functions as an NTPase, an RTPase, or both within cores. The λ1 shell protein has been proposed to be the capping RTPase in cores based on its reported *in vitro* RTPase activity (12). However, given our new evidence for *in vitro* RTPase activity of μ2, there appears to be little reason from enzymatic or genetic data to conclude that λ1 is more likely than μ2 to represent the capping RTPase. The apparent K_m values for RNA substrate reported for λ1 and μ2 are similarly low (0.26 and 0.32 μm, respectively), although the reported K_{cat} of the λ1-RNA reaction (3.1 min^{-1}) is 10-fold higher than that of the μ2-RNA reaction (0.3 min^{-1}) (Ref. 12; this study, Table II). An *in vitro* system for coupled transcription and capping reconstituted from wt or mutant mORV proteins would be useful for dissecting the relative roles of λ1 and μ2 but has not been reported to date. We are currently testing core-like particles assembled in insect cells from baculovirus-expressed mORV proteins (39)[3] for this purpose. New information about the precise structural positions and orientations of proteins within the core may also be informative since whether the catalytic regions of λ1 or μ2 have access to the triphosphorylated 5′ end of nascent mRNA within the crowded core interior may be a key determinant of whether either protein truly acts as an RTPase during viral mRNA synthesis (4, 9, 10).[4]

What other types of functions might μ2 or λ1 mediate that could be associated with NTP hydrolysis? Many enzymes are known to couple NTP hydrolysis to protein conformational changes; RNA and DNA helicases, myosins, kinesins, and G proteins are well known examples. In many cases the conformational changes allow movement of the NTPase along a nucleic acid or protein polymer track (53, 54). The λ3 crystal structure suggests some such possible roles for μ2 or λ1 in melting, translocating, and/or reannealing the genomic plus-strand RNA as it is passed around the outside of the λ3 polymerase, whereas the genomic minus-strand RNA is passed through the central cavity (and catalytic site) of λ3 during transcript elongation (9). Alternatively, an NTP-dependent activity by either μ2 or λ1 could be required during a limited part of each transcription cycle, such as for template melting or translocation before the transcript has reached a certain length or for reinitiation after termination. To understand the functions of the mORV core as a molecular machine for mRNA synthesis, the roles of μ2 and λ1 must be characterized in more detail. The capacity of μ2 to bind to microtubules (this study, Fig. 3*B*; also see Refs. 35 and 36) dictates that we must also be alert to possible NTP-dependent functions of μ2 during mORV genome replication and assembly in infected cells.

Acknowledgments—We thank Elaine Freimont and Jason Dinoso for excellent technical support, Yizhi Tao and Steve Harrison for advice about λ3 purification, Teresa Broering for use of her μNS antiserum and expression constructs, Michael Farzan and Steve Buratowski for suggestions about enzyme assays, and other members of our laboratory for helpful discussions. We also thank Teresa Broering and Cathy Miller for reviewing preliminary drafts of the manuscript.

REFERENCES

1. Nibert, M. L. (1998) *Curr. Top. Microbiol. Immunol.* **233,** 1–30
2. Nibert, M. L., and Schiff, L. A. (2001) in *Fields Virology* (Knipe, D. M., and Howley, P. M., eds) 4th Ed., pp. 1679–1728, Lippincott Williams & Wilkins, Philadelphia
3. Yue, Z., and Shatkin, A. J. (1998) *Curr. Top. Microbiol. Immunol.* **233,** 31–56
4. Reinisch, K. M., Nibert, M. L., and Harrison, S. C. (2000) *Nature* **404,** 960–967
5. Dryden, K. A., Farsetta, D. L., Wang, G., Keegan, J. M., Fields, B. N., Baker, T. S., and Nibert, M. L. (1998) *Virology* **245,** 33–46
6. Drayna, D., and Fields, B. N. (1982) *J. Virol.* **41,** 110–118
7. Morozov, S. Y. (1989) *Nucleic Acids Res.* **17,** 5394
8. Starnes, M. C., and Joklik, W. K. (1993) *Virology* **193,** 356–366
9. Tao, Y., Farsetta, D. L., Nibert, M. L., and Harrison, S. C. (2002) *Cell* **111,** 733–745
10. Zhang, X., Walker, S. B., Chipman, P. R., Nibert, M. L., and Baker, T. S. (2003) *Nat. Struct. Biol.* **10,** 1011–1018
11. Furuichi, Y., Muthukrishnan, S., Tomasz, J., and Shatkin, A. J. (1976) *Prog. Nucleic Acid Res. Mol. Biol.* **19,** 3–20
12. Bisaillon, M., and Lemay, G. (1997) *J. Biol. Chem.* **272,** 29954–29957
13. Bujnicki, J. M., and Rychlewski, L. (2001) *Genome Biology* http://genomebiology.com/2001/2/9/RESEARCH/0038
14. Cleveland, D. R., Zarbl, H., and Millward, S. (1986) *J. Virol.* **60,** 307–311
15. Fausnaugh, J., and Shatkin, A. J. (1990) *J. Biol. Chem.* **265,** 7669–7672
16. Luongo, C. L., Contreras, C. M., Farsetta, D. L., and Nibert, M. L. (1998) *J. Biol. Chem.* **273,** 23773–23780
17. Luongo, C. L., Reinisch, K. M., Harrison, S. C., and Nibert, M. L. (2000) *J. Biol. Chem.* **275,** 2804–2810
18. Mao, Z. X., and Joklik, W. K. (1991) *Virology* **185,** 377–386
19. Bartlett, N. M., Gillies, S. C., Bullivant, S., and Bellamy, A. R. (1974) *J. Virol.* **14,** 315–326
20. Gillies, S., Bullivant, S., and Bellamy, A. R. (1971) *Science* **174,** 694–696
21. Borsa, J., Grover, J., and Chapman, J. D. (1970) *J. Virol.* **6,** 295–302
22. Kapuler, A. M., Mendelsohn, N., Klett, H., and Acs, G. (1970) *Nature* **225,** 1209–1213
23. Noble, S., and Nibert, M. L. (1997) *J. Virol.* **71,** 2182–2191
24. Noble, S., and Nibert, M. L. (1997) *J. Virol.* **71,** 7728–7735
25. Jin, J., Dong, W., and Guarino, L. A. (1998) *J. Virol.* **72,** 10011–10019
26. Martins, A, and Shuman, S. (2003) *Nucleic Acids Res.* **31,** 1455–1463
27. Myette, J. R., and Niles, E. G. (1996) *J. Biol. Chem.* **271,** 11945–11952
28. Vasiljeva, L., Merits, A., Auvinen, P., and Kaariainen, L. (2000) *J. Biol. Chem.* **275,** 17281–17287

29. Yu, L., and Shuman, S. (1996) *J. Virol.* **70,** 6162–6168
30. Bisaillon, M., Bergeron, J., and Lemay, G. (1997) *J. Biol. Chem.* **272,** 18298–18303
31. Yin, P., Cheang, M., and Coombs, K. M. (1996) *J. Virol.* **70,** 1223–1227
32. Bisaillon, M., and Lemay, G. (1997) *Virus Res.* **51,** 231–237
33. Brentano, L., Noah, D. L., Brown, E. G., and Sherry, B. (1998) *J. Virol.* **72,** 8354–8357
34. Lemay, G., and Danis, C. (1994) *J. Gen. Virol.* **75,** 3261–3266
35. Parker, J. S. L., Broering, T. J., Kim, J., Higgins, D. E., and Nibert, M. L. (2002) *J. Virol.* **76,** 4483–4496
36. Broering, T. J., Parker, J. S. L., Joyce, P. L., Kim, J., and Nibert, M. L. (2002) *J. Virol.* 8285–8297
37. Becker, M. M., Goral, M. I., Hazelton, P. R., Baer, G. S., Rodgers, S. E., Brown, E. G., Coombs, K. M., and Dermody, T. S. (2001) *J. Virol.* **75,** 1459–1475
38. Mbisa, J. L., Becker, M. M., Zou, S., Dermody, T. S., and Brown, E. G. (2000) *Virology* **272,** 16–26
39. Kim, J., Zhang, X., Centonze, V. E., Bowman, V. D., Noble, S., Baker, T. S., and Nibert, M. L. (2002) *J. Virol.* **76,** 12211–12222
40. Farsetta, D. L. (2000) *Mammalian Orthovrovirus Transcription: The Architecture of Transcriptional Enzymes and the Regulation of Transcriptional Initiation and Elongation*. Ph.D. thesis, University of Wisconsin, Madison, WI
41. Attoui, H., Fang, Q., Jaafar, F. M., Cantaloube, J. F., Biagini, P., De Micco, P., and De Lamballerie, X. (2002) *J. Gen. Virol.* **83,** 1941–1951
42. Rikkonen, M., Peranen, J., and Kaariainen, L. (1994) *J. Virol.* **68,** 5804–5810
43. Coombs, K. M. (1996) *J. Virol.* **70,** 4237–4245
44. Gustke, N., Trinczek, B., Biernat, J., Mandelkow, E. M., and Mandelkow, E. (1994) *Biochemistry* **33,** 9511–9522
45. Walenta, J. H., Didier, A. J., Liu, X., and Kramer, H. (2001) *J. Cell Biol.* **152,** 923–934
46. Haller, B. L., Barkon, M. L., Vogler, G. P., and Virgin, H. W., IV. (1995) *J. Virol.* **69,** 357–364
47. Nibert, M. L., Furlong, D. B., and Fields, B. N. (1991) *J. Clin. Invest.* **88,** 727–734
48. Sherry, B., and Blum, M. A. (1994) *J. Virol.* **68,** 8461–8465
49. Banerjee, A. K., Ward, R., and Shatkin, A. J. (1971) *Nat. New Biol.* **230,** 169–172
50. Bentley, D. (2002) *Curr. Opin. Cell Biol.* **14,** 336–342
51. Proudfoot, N. J., Furger, A., and Dye, M. J. (2002) *Cell* **108,** 501–512
52. Gross, C. H., and Shuman, S. (1996) *J. Virol.* **70,** 1706–1713
53. Patel, S. S., and Picha, K. M. (2000) *Annu. Rev. Biochem.* **69,** 651–697
54. Sablin, E. P., and Fletterick, R. J. (2001) *Curr. Opin. Struct. Biol.* **11,** 716–724
55. Wiener, J. R., Bartlett, J. A., and Joklik, W. K. (1989) *Virology* **169,** 293–304
56. Zou, S., and Brown, E. G. (1992) *Virus Res.* **22,** 159–164

Nucleoside and RNA Triphosphatase Activities of Orthoreovirus Transcriptase Cofactor μ2

Jonghwa Kim, John S. L. Parker, Kenneth E. Murray and Max L. Nibert

J. Biol. Chem. 2004, 279:4394-4403.
doi: 10.1074/jbc.M308637200 originally published online November 12, 2003
